requirement that ℓ in Eq. (4d) should be real, we obtain, after some lengthy but straightforward algebra,

$$k^2 \le \frac{\omega^2}{a_0^2 - u_0^2} + \left(\frac{2\Omega}{a_0}\right)^2 \left[-1 + \left(\frac{a_0 k}{\omega}\right)^2 (1 - M_0^2)^2 + \left(\frac{2\Omega}{\omega}\right)^2 M_0^2 \left(\frac{a_0 k}{\omega}\right)^4 (1 - M_0^2)^5 + O\left(\frac{2\Omega}{\omega}\right)^3 \right] \tag{7}$$

where $M_0 = u_0/a_0$; the expression is valid for $2\Omega/\omega \ll 1$, or below Coriolis resonance. On the right-hand side of the inequality just given, the second term represents the effect of rotation, which, obviously, is absent for a nonrotating duct.

The confirmation of the present predictions, either by elaborate numerical procedure or experiments, remains to be settled.

Acknowledgments

The work is supported by NASA Lewis Research Center, under Contract NASA NAG 3-86 with Dr. W. Rostafinsky as a technical monitor.

References

[1] Goldstein, M. E., *Aeroacoustics*, McGraw-Hill Book Co., New York, 1976.

[2] Görtler, H., "Einige Bemerkungen über Strömungen in rotierenden Flüssigkeiten," *Zeitschrift der Angewandte Mathematik und Mechanik*, Vol. 24, No. 5, 1944, pp. 210-214.

[3] Görtler, H., "On Forced Scillations in Rotating Fluids," *Proceedings of the Fifth Midwestern Conference on Fluid Mechanics*, University of Michigan Press, Ann Arbor, Mich., 1957, pp. 1-10.

[4] Greenspan, H. P., *The Theory of Rotating Flows*, Cambridge University Press, Cambridge, England, 1968, p. 3.

AIAA 82-4192

Pressure Distributions and Shock Shapes for a Bent-Nose Biconic at Incidence

Charles G. Miller III* and Peter A. Gnoffo*
NASA Langley Research Center, Hampton, Va.

Nomenclature

L	= model length, m
N_{Re}	= unit Reynolds number, m^{-1}
p	= pressure, N/m^2
y,z	= coordinates (see Fig. 1)
α	= angle of attack, deg
θ	= cone half angle, deg
ϕ	= circumferential angle, deg ($\phi = 180$ deg is most windward ray and $\phi = 0$ deg is most leeward ray)

Subscripts

f	= fore cone
m	= measured
∞	= freestream conditions
s	= surface

Received Sept. 3, 1981; revision received Dec. 9, 1981.

*Aero-Space Technologist, Aerothermodynamics Branch, Space Systems Division. Member AIAA.

Introduction

FEASIBILITY studies of the aerocapture and aerobraking techniques[1-3] for proposed flights to Mars, Venus, Saturn, and Titan demonstrate that the biconic shape offers the best combination of high lift-to-drag ratio for inserting accuracy, low hypersonic ballistic coefficient, and high volumetric efficiency. Also, biconic shapes would fit nicely into the shuttle orbiter bay. The leading candidate emerging from these feasibility studies[2,3] is a 12.84/7 deg biconic with the fore-cone section bent upward relative to the aft-cone section. To assist in the establishment of an accurate hypersonic data base for this proposed configuration, a study has been initiated at the Langley Research Center. The purpose of this Note is to present the initial results of this experimental study and make comparisons to prediction. These results include pressure distributions and shock shapes measured on a spherically blunted bent-nose biconic model at Mach 6 in air for angles of attack from 0 to 25 deg.

Apparatus and Tests

The present study was performed in the Langley 20-in. Mach 6 tunnel.[4] Reservoir pressure and temperature were 3.5 MN/m^2 and 500 K, respectively, corresponding to a freestream Mach number of 6.0 and unit Reynolds number of 28.7×10^6/m in ideal air.

A planform view of the bent-nose biconic model is shown in Fig. 1. This model has a fore-cone half-angle of 12.84 deg, aft-cone half-angle of 7 deg, spherical nose radius of 5.79 mm, and base radius of 3.81 cm. The fore cone is bent upward 7 deg relative to the aft cone. Sixty-two surface pressure orifices were distributed along five rays (the most windward, most leeward, and three rays at 45-deg increments between the windward and leeward rays) and two orifices were located on the base. The model was mounted with a 2.54-cm-diam sting and the ratio of sting length to diameter exceeded 7. Tests were performed over a range of angle of attack α from 0 to 25 deg in 5-deg increments, where α is referenced to the axis of the aft-cone section. The angle of attack was read from the schlieren photographs.

Pressures were measured using variable capacitance diaphragm transducers and the output recorded by an analog-to-digital system. Shock shapes were recorded using a single pass schlieren system. These shock shapes were read manually from enlargements of schlieren photographs to approximately 1.4 times actual model size.

Prediction

Pressure distributions and shock shapes were computed using a steady, three-dimensional, inviscid flowfield code.[5] This code, referred to as STEIN (supersonic three-dimensional external inviscid), uses a MacCormack-like scheme to integrate the three-dimensional Euler equations. Shock waves are computed as discontinuities via the Rankine-Hugoniot jump conditions. The Mach number in the marching direction (an axis running from the nose of the vehicle to the base) must be supersonic at every point in the flowfield, and the geometry such that no embedded regions of subsonic flow exist. The subsonic-supersonic flow about the spherical nose was computed using a blunt body code.[6]

Results and Discussion

Measured and predicted shock shapes are presented in Fig. 1 for various angles of attack. The most upstream inflection in the measured windward shock is due to an overexpansion of the flow from the spherical nose.[7] The second inflection on the windward side is due to the flow expansion occurring at the fore-cone/aft-cone junction. The point at which the windward shock turns inward due to the junction moves slowly toward the nose with angle of attack. For $\alpha_m \ge 21$ deg, the windward shock just upstream of the base has become parallel to the aft-cone surface. Shock detachment distance on

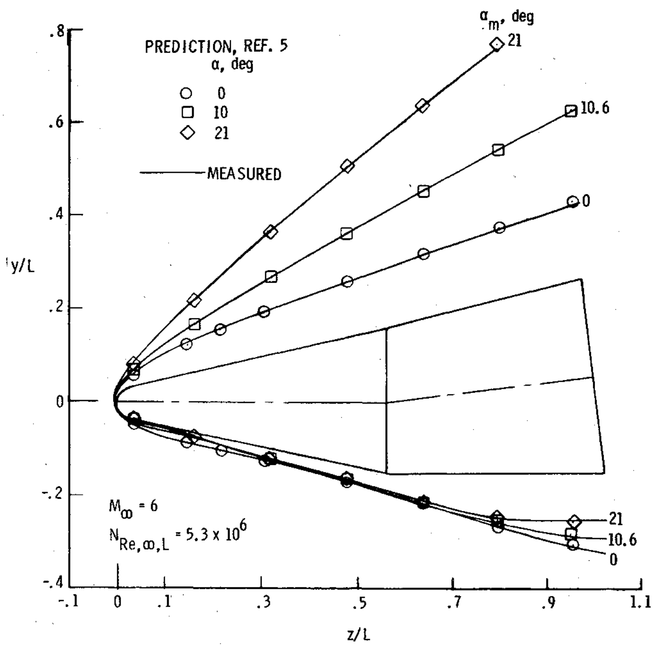

Fig. 1 Effect of angle of attack on shock shape.

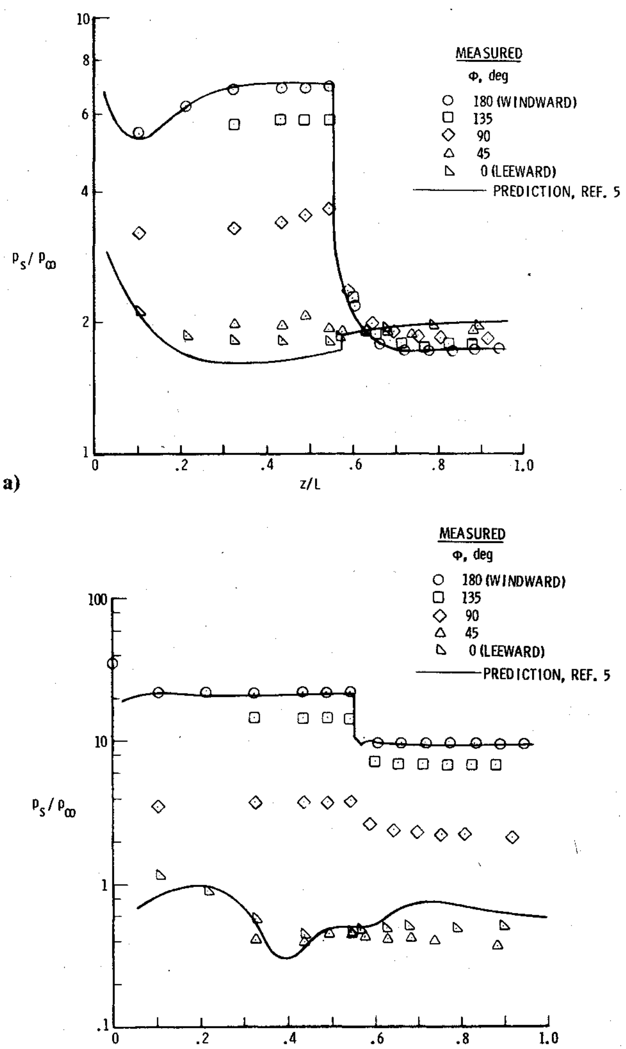

Fig. 2 Pressure distribution at angles of attack; $M_\infty = 6$, $N_{Re,\infty,L} = 5.3 \times 10^6$; a) $\alpha_m = 0$ deg, b) $\alpha_m = 21$ deg.

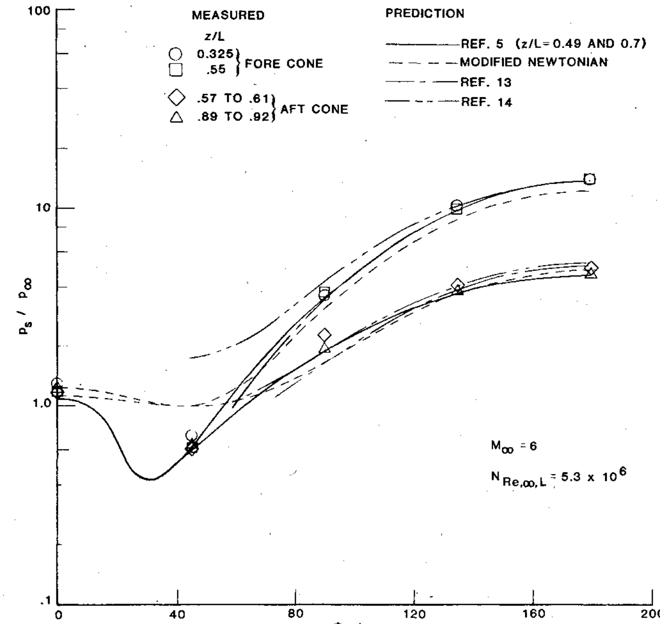

Fig. 3 Circumferential pressure distributions at $\alpha_m = 10.6$ deg.

the leeward side shows no effect of the junction and is more sensitive to α than the detachment distance on the windward side. For values of z/L greater than 0.4, the leeward shock angle relative to the fore-cone axis is approximately $\theta_f + \alpha_f$. Measured and predicted (STEIN code) shock shapes were observed to agree to within 3% for all angles of attack.

For fore-cone angles of attack α_f exceeding the fore-cone half-angle θ_f, the schlieren photographs revealed the existence of an embedded shock on the leeward side. This shock originates on the fore-cone section just downstream of the sphere-cone junction ($z/L \approx 0.036$ at $\alpha_m = 21$ deg). For values of z/L between 0.3 and 0.8, the embedded shock was inclined approximately $\alpha_f + 11$ deg with the fore-cone axis.

Measured and predicted surface pressure distributions are shown in Fig. 2 for angles of attack of 0 and 21 deg. The overexpansion of the flow from the spherical nose on the windward side diminishes with α_m, as expected,[7] and is predicted quite well by the STEIN code. For $\alpha_m > 5$ deg, the windward aft-cone pressures were observed to be essentially constant with z/L and also predicted by STEIN. At $\alpha_m = 0$ deg, the STEIN code accurately predicts the measured monotonic decrease in p_s/p_∞ just downstream of the fore-cone/aft-cone junction. (Similar comparisons[8,9] for an on-axis biconic show that STEIN is only in fair agreement with measured data just downstream of the junction and a more accurate description of measurement is provided by a numerical method using the parabolized Navier-Stokes equations.)

For values of α corresponding to the leeward side being nearly shielded or fully shielded from the flow ($\alpha_f \geq \theta_f$), the measured leeward p_s/p_∞ at $\phi = 0$ deg exceeds that at $\phi = 45$ deg. This minimum in the circumferential pressure distribution is shown in Fig. 3 for $\alpha_m = 10.6$ deg and has been observed in previous cone studies.[10-12] It is attributed to the flow separating on the leeward side and forming two symmetrical, supersonic, counter-rotation longitudinal vortices with an attachment line on the most leeward ray. The origin of this leeward separated flow region occurs closer to the nose with increasing α.[11,12] The predicted circumferential pressure distribution from STEIN is in good agreement with measurement. For the present range of α_m, the leeward surface pressure immediately upstream of the base exceeded the measured leeward base pressure, implying no significant communication between the two flow regions.

References

[1]French, J. R. and Cruz, M. I., "Aerobraking and Aerocapture for Planetary Missions," *Astronautics & Aeronautics*, Feb. 1980, pp. 48-55, and 71.

[2]Florence, D. E., "Aerothermodynamic Design Feasibility of a Mars Aerocapture/Aeromaneuver Vehicle," AIAA Paper 81-0350, Jan. 1981.

[3]Florence, D. E., "Aerothermodynamic Design Feasibility of a Generic Planetary Aerocapture/Aeromaneuver Vehicle," AIAA Paper 81-1127, June 1981.

[4]Goldberg, T. J. and Hefner, J. N., "Starting Phenomena for Hypersonic Inlets with Thick Turbulent Boundary Layers at Mach 6," NASA TN D-6280, Aug. 1971.

[5]Marconi, F., Salas, M., and Yaeger, L., "Development of a Computer Code for Calculating the Steady Super/Hypersonic Inviscid Flow Around Real Configurations. Volume I—Computational Technique," NASA CR-2675, April 1976.

[6]Moretti, G. and Bleich, G., "Three-Dimensional Flow Around Blunt Bodies," *AIAA Journal*, Vol. 5, Sept. 1967, pp. 1557-1562.

[7]Cleary, J. W., "Effects of Angle of Attack and Nose Bluntness on the Hypersonic Flow Over Cones," AIAA Paper 66-414, June 1966.

[8]Helliwell, W. S., Dickinson, R. P., and Lubard, S. C., "Viscous Flow Over Arbitrary Geometries at High Angle of Attack," *AIAA Journal*, Vol. 19, Feb. 1981, pp. 191-197.

[9]Mayne, A., "Calculation of the Laminar Viscous Shock Layer on a Blunt Biconic Body at Incidence to Supersonic and Hypersonic Flow," AEDC-TR-76-123, Dec. 1976.

[10]Lubard, S. C. and Helliwell, W. S., "Calculation of the Flow on a Cone at High Angle of Attack," *AIAA Journal*, Vol. 12, July 1974, pp. 965-974.

[11]Stetson, K. R., "Boundary-Layer Separation on Slender Cones at Angle of Attack," *AIAA Journal*, Vol. 10, May 1972, pp. 642-648.

[12]Rainbird, W. J., "Turbulent Boundary-Layer Growth and Separation on a Yawed Cone," *AIAA Journal*, Vol. 6, Dec. 1968, pp. 2410-2416.

[13]Amick, J. L., "Pressure Measurements on Sharp and Blunt 5°- and 15°-Half-Angle Cones at Mach Number 3.86 and Angles of Attack to 100°," NASA TN D-753, Feb. 1961.

[14]High, M. D. and Blick, E. F., "Cone Pressure Distribution at Large and Small Angles of Attack," *AIAA Journal*, Vol. 2, Nov. 1964, pp. 2054-2055.